



Article citation info:

Liu D, Sun N, Zhu G, Cao H, Wang T, Li G, Gu F, Modelling and evaluating piston slap-induced cavitation of cylinder liners in heavy-duty diesel engines, *Eksploatacja i Niezawodność – Maintenance and Reliability* 2023: 25(3) <http://doi.org/10.17531/ein/169644>

## Modelling and evaluating piston slap-induced cavitation of cylinder liners in heavy-duty diesel engines

Indexed by:



Dong Liu<sup>a</sup>, Nannan Sun<sup>b</sup>, Guixiang Zhu<sup>b</sup>, Hengchao Cao<sup>b</sup>, Tie Wang<sup>a,\*</sup>, Guoxing Li<sup>a</sup>, Fengshou Gu<sup>c</sup>

<sup>a</sup> Department of Vehicle Engineering, Taiyuan University of Technology, Taiyuan 030024, China

<sup>b</sup> Weichai Power Co., Ltd., Weifang 261061, China

<sup>c</sup> Centre for Efficiency and Performance Engineering, University of Huddersfield HD1 3DH, United Kingdom

### Highlights

- A quantitative assessment method for cylinder liner cavitation risk is proposed.
- There is a nonlinear relationship between liner vibration and coolant pressure.
- The thin liquid layer will lower the threshold for triggering cavitation.
- Cylinders with higher mode shape coefficients have a higher risk of cavitation.
- Reducing piston-liner clearance and proper piston pin offset can help reduce the cavitation risk.

### Abstract

Cavitation erosion of cylinder liner seriously affects the operational reliability and service life of heavy-duty diesel engines. The accuracy of the modeling-based cavitation risk evaluation is limited by the unclear correspondence between cylinder liner vibration and coolant cavitation. This report is intended to investigate the correspondence between cylinder liner vibration and coolant pressure by combining vibration cavitation test, pressure gradient calculation, and visualization observation. The cavitation risk of the cylinder liner under the piston slap is quantitatively analyzed based on a nonlinear structural dynamics model that incorporates the piston-cylinder liner nonlinear collision, piston thermal deformation, and preload of cylinder head. The results show that the occurrence of cavitation will cause a nonlinear relationship between the cylinder liner acceleration and the coolant pressure. The engine under study has a high risk of cavitation when the cylinder liner acceleration exceeds  $1189 \text{ m/s}^2$ . The difference in cavitation risk for each cylinder is related to the structural modal characteristics of the crankcase. In addition, the effect of piston-liner clearance and piston pin offset on the cavitation risk is investigated based on the dynamics model.

### Keywords

heavy-duty diesel engines, cavitation evaluation, dynamics model, liner acceleration, coolant pressure.

This is an open access article under the CC BY license (<https://creativecommons.org/licenses/by/4.0/>)

### 1. Introduction

Heavy-duty diesel engines are the main power source for commercial vehicles, construction machinery, agricultural machinery, ships, power generation equipment and defense equipment [18, 28]. In recent years, with the increasing average effective pressure and power of diesel engines, the structure of diesel engines tends to be more compact, which has increased

the cavitation risk of cylinder liners to a large extent [5, 23, 33]. Cavitation will occur when the coolant pressure is lower than the saturated vapor pressure. The cavitation erosion of the cylinder liner is generated by the pulse pressure and micro-jet impact following the collapse of cavitation bubbles [27, 29]. Once cavitation erosion happens, the cylinder liner will

(\*) Corresponding author.

E-mail addresses:

D. Liu (ORCID: 0009-0000-3574-5297) [liudong9512@163.com](mailto:liudong9512@163.com), N. Sun, [sunnann@weichai.com](mailto:sunnann@weichai.com), G. Zhu, [zhugx@weichai.com](mailto:zhugx@weichai.com), H. Cao, [caohengchao@weichai.com](mailto:caohengchao@weichai.com), T. Wang (ORCID: 0000-0002-8842-0813) [wangtie57@163.com](mailto:wangtie57@163.com), G. Li (ORCID: 0000-0002-6813-3294) [liguoxing@tyut.edu.cn](mailto:liguoxing@tyut.edu.cn), F. Gu (ORCID: 0000-0003-4907-525X) [f.gu@hud.ac.uk](mailto:f.gu@hud.ac.uk)

probably fail earlier than its expected lifespan, seriously affecting the reliability and service life of heavy-duty diesel engines [1, 4, 14]. In order to ensure the stable operation of heavy-duty diesel engines within the rated life, it is of great significance to analyze the mechanism of cavitation caused by cylinder liner vibration and accomplish the early evaluation of the cavitation risk of cylinder liners.

The high-frequency vibration of the cylinder liner is the origin of cavitation, and the calculation of the dynamic response of the cylinder liner is the basis of cavitation risk evaluation. Meng [20] and Tsujiuchi et al. [30] developed dynamics models based on the analytical method to predict the piston secondary motion and cylinder liner vibration, which models the cylinder liner as a spring-mass system. Geng [11] and Dolatabadi et al. [7] developed two-degree-of-freedom nonlinear dynamics models to predict the occurrence timing and frequency of piston slap on the cylinder liner. In order to calculate the dynamic response of the cylinder liner in three dimensions, the researchers calculated the contact force between the piston and the cylinder liner by the analytical method and used it as the input boundary of the finite element model [8, 26, 35]. Theoretical-based calculations can provide a simple solution. However, the results cannot be directly used for cavitation risk evaluation due to the limited degrees of freedom, difficulty defining boundary constraints, and lack of structural characteristics. In order to obtain more accurate and reliable simulation results, multi-body dynamics (MBD) and finite element method (FEM) has received attention in this field. Gomboc et al. [12] developed a multi-body dynamics model of the cylinder assembly to simulate the dynamic behavior of the cylinder liner through the elastic piston-liner contact. Murakami et al. [22] analyzed the piston secondary motion by the finite element method and studied the effect of piston structural parameters on the skirt stress and cylinder liner vibration amplitude. Li et al. [16] investigated the relationship between the combustion behavior and the frequency response of the cylinder liner based on an improved finite element model. However, most current research has been conducted based on quasi-static models. These models ignore the nonlinear contact and collision behavior between the piston and the cylinder liner, which cannot simulate the repeated contact and elastic deformation between them. In addition, these studies have

mainly focused on the dynamic characteristics of individual cylinders, the structural characteristics of the crankcase and its contact constraints with the cylinder liner have been oversimplified or neglected, and the vibration differences between each cylinder of multi-cylinder diesel engines have rarely been studied.

The generation and development of cavitation erosion is an extremely complex phenomenon [10, 24]. Researchers have tried to develop methods and numerical models for predicting cylinder liner cavitation erosion over the past decades. Low [19] and Hosny et al. [13] defined the cavitation safety factor (CSF) based on the ratio of the critical cavitation velocity (CCV) to the calculated wall velocity. Peiyou [26] calculated the local peak acceleration of the cylinder liner based on the combination of the analytical formulation and finite element method introduced in the previous paper, which was compared with the cavitation failure area in the actual case. Zhang [36] and Lin et al. [17] used computational fluid dynamics (CFD) methods to calculate the gas volume fraction distribution of the coolant, which uses the cylinder liner vibration as the motion boundary of the flow field. Obviously, the above models are more suitable for post-failure analysis and trending studies due to the lack of accurate dynamics simulations with the critical cavitation evaluation parameters. To achieve a more comprehensive evaluation, Gomboc et al. [12] predicted the cavitation risk of the cylinder liner by coupling computational fluid dynamics with multi-body dynamics. Wang et al. [32, 34] proposed an acoustic-solid coupling method to study the correlation between acoustic characteristics of coolant passage and pressure fluctuation, which focuses more on global pressure fluctuation and does not involve local pressure distribution and cavitation risk area prediction.

Up to now, due to the complexity of the vibrational cavitation behavior and the lack of reliable physical models for cavitation prediction, most studies have focused on the post-failure analysis and the effects of a wide range of parameters on cavitation erosion. On the one hand, most existing models did not consider the coupled dynamic behavior between the piston and the cylinder liner, and ignored the influence of the crankcase structural constraints on the cylinder liners. On the other hand, due to the unclear correspondence between cylinder liner vibration and cavitation, existing cavitation evaluation models

cannot provide reliable quantitative indicators, which further limited the accuracy of cavitation evaluation based on dynamics simulation.

This study aims to determine the quantitative relationship between vibration and cavitation and to achieve a quantitative evaluation of the cavitation risk of the cylinder liner. The nonlinear relationship between cylinder liner acceleration and coolant pressure is investigated experimentally, and the cavitation threshold is defined by the derived cavitation number equation. A structural dynamics model considering structural modal properties, nonlinear contact constraints and time-varying excitation is developed and experimentally verified. The cavitation risk of each cylinder of the heavy-duty diesel engine is analyzed based on simultaneous solution of the piston secondary motion and cylinder liner vibration. In addition, the effect of piston-liner clearance and piston pin offset on the dynamic characteristics of the cylinder liner and the cavitation risk is investigated. The method and model proposed in this study can effectively evaluate the cavitation risk of cylinder liners and provide a valuable reference for cavitation prediction and mitigation studies in heavy-duty diesel engines.

## 2. Theories of cylinder dynamics and cavitation evaluation

The critical to cavitation prediction is the accurate simulation of cylinder liner vibration and cavitation evaluation criteria. This section introduces the finite element solution theory for the piston secondary motion and derives the acceleration-based cavitation number equation.

### 2.1. Piston-liner dynamics

In order to reconstruct the contact behavior between the piston skirt and the cylinder liner, this paper uses the finite element method to solve for the piston secondary motion. The structural components are discretized according to the finite element theory. Then the motion equation of the dynamics model is as follows:

$$[M]\{\ddot{u}(t)\} + [C]\{\dot{u}(t)\} + [K]\{u(t)\} = \{F(t)\} \quad (1)$$

where  $[M]$ ,  $[C]$  and  $[K]$  are the mass matrix, damped matrix and stiffness matrix,  $\{u(t)\}$ ,  $\{\dot{u}(t)\}$  and  $\{\ddot{u}(t)\}$  are the displacement, velocity and acceleration vectors,  $t$  is the time,  $F(t)$  is the load vector applied on the unit.

Discretizing equation (1) by the Newmark time integration algorithm, the iterations of displacement and velocity are as

follows [31]:

$$\{\dot{u}_{n+1}\} = \{\dot{u}_n\} + [(1 - \delta)\{\dot{u}_n\} + \delta\{\dot{u}_{n+1}\}]\Delta t \quad (2)$$

$$\{u_{n+1}\} = \{u_n\} + \{\dot{u}_n\}\Delta t + \left[\left(\frac{1}{2} - \alpha\right)\{\ddot{u}_n\} + \alpha\{\ddot{u}_{n+1}\}\right]\Delta t^2 \quad (3)$$

where  $\alpha$  and  $\delta$  are the Newmark's integration parameters.

Substitute Eq.2 and Eq.3 into Eq.1:

$$\begin{aligned} & \left(\frac{1}{\alpha\Delta t^2}[M] + \frac{\delta}{\alpha\Delta t}[C] + [K]\right)\{u_{n+1}\} \\ & = \{F_{n+1}\} + [M]\left(\frac{1}{\alpha\Delta t^2}\{u_n\} + \frac{1}{\alpha\Delta t}\{\dot{u}_n\} + \frac{1-2\alpha}{2\alpha}\{\ddot{u}_n\}\right) \\ & + [C]\left(\frac{\delta}{\alpha\Delta t}\{u_n\} + \frac{\delta-\alpha}{\alpha}\{\dot{u}_n\} + \frac{\Delta t}{2}\left(\frac{\delta}{\alpha}-2\right)\{\ddot{u}_n\}\right) \end{aligned} \quad (4)$$

As the cylinder liner is subjected to the cylinder head preload, the initial displacement  $\{u_0\}$  is derived from the static calculation as:

$$[k]\{u_0\} = \{F\} \quad (5)$$

The initial velocity  $\{\dot{u}_n\}$  and the initial acceleration  $\{\ddot{u}_n\}$  are set to 0, and then the dynamic response of units in the system can be solved using Eq.4.

### 2.2. Cavitation evaluation of cylinder liner

Cavitation onset in a high-speed flow can be characterized using a variant of the Euler number known as the cavitation number [6]. The cavitation number is typically of the form

$$Ca = \frac{p_r - p_v}{\frac{1}{2}\rho v^2} \quad (6)$$

where  $p_r$  is the reference pressure,  $p_v$  is the saturation vapor pressure,  $\rho$  is the liquid density, and  $v$  is the local velocity .

However, the conventional cavitation number ( $Ca$ ) could incorrectly predict the cavitation onset in a liquid accelerated in a short amount of time [25]. The velocity peak of the cylinder liner is around 0.1m/s, and the acceleration peak might be higher than 1000m/s<sup>2</sup>. Therefore, this equation is rarely used for cavitation risk evaluation of cylinder liners. A more widely used cavitation safety factor equation is as follows:

$$CSF = \frac{V_{ccv}}{V_{max}} \quad (7)$$

where  $V_{max}$  is the maximum vibration velocity of the cylinder liner;  $V_{ccv}$  is the cavitation critical velocity, which is derived from the following empirical equation:

$$p_s - p_v = \rho c V_{ccv} \quad (8)$$

where  $p_s$  is the coolant static pressure;  $c$  is the speed of sound in the coolant.

However, this empirical formula cannot consider the pressure gradient of the cooling water jacket in the thickness direction. In addition, the water jacket thickness of heavy-duty diesel engines is usually less than 5mm, and the thin liquid layer configuration will lead to a large amplification of the pressure [3]. Therefore, Eq.7 is more applicable to the post-failure analysis.

This paper introduces the cavitation number equation considering acceleration and pressure gradient in the cavitation risk evaluation of the cylinder liner [25]. The new cavitation number is based on the assumption that the liquid is inviscid and incompressible and has a velocity magnitude significantly smaller than the acceleration ( $\partial v/\partial t$ ), as is commonly known [2, 15], only the pressure gradient and acceleration remain, and the Navier–Stokes equations are reduced to

$$\frac{\partial v}{\partial t} = -\frac{1}{\rho}\nabla p \quad (9)$$

Integrating Eq.9 along the liquid from the cylinder liner to the crankcase (assuming the thickness of the cooling water jacket is  $h$ ), denoting the magnitude of the vertical component of  $\partial v/\partial t$  as  $a$ , and solving for the pressure difference in the direction of liner vibration.

$$p_r - p_l = \rho ah \quad (10)$$

where  $p_r$  is the reference pressure which also refers to the water pressure on the crankcase surface,  $p_l$  is the pressure at the liner surface. Cavitation is likely to occur when  $p_l < p_v$ . Thus, we can establish

$$Ca = \frac{p_r - p_v}{\rho ah} \quad (11)$$

as an indicator of cavitation onset when the flow undergoes a violent acceleration. In this equation, cavitation is likely to occur when  $Ca < 1$ .

In particular, due to the high-frequency vibration of the cylinder liner and the narrower cooling water jacket, the reference pressure  $p_r$  in Eq.11 is no longer a constant value but constantly varies with the cylinder liner vibration. Therefore, it is necessary to obtain the acceleration of the cylinder liner and the cooling water pressure at the crankcase simultaneously by installing sensors to enable the evaluation of the cavitation risk on the cylinder liner surface.

### 3. Test and simulation

The research presented in this paper utilized a methodology that

integrated both experimental and numerical simulation techniques, as detailed in Figure 1. Through impact vibration tests, the acceleration threshold for cavitation was determined by the combination of pressure measurements and the cavitation number equations. The engine bench test furnished input parameters such as combustion pressure and speed for the dynamics model, and the model was further validated through the measured cylinder liner acceleration signals.

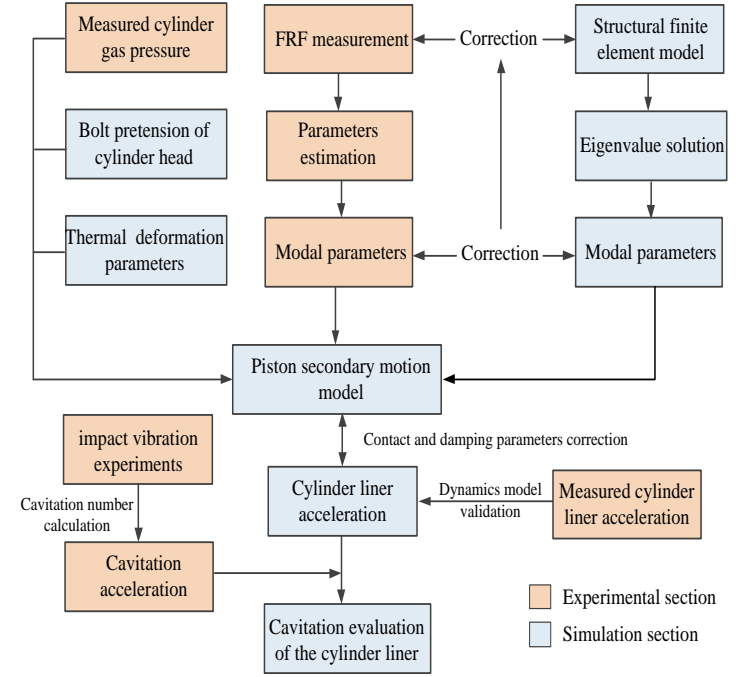


Fig.1. The cavitation evaluation model developed in this paper.

#### 3.1. Test design

The studied engine is a heavy-duty diesel engine with 4 cycles, 6 cylinders and a displacement of 8.8 dm<sup>3</sup>. The firing order of this diesel engine is 1-5-3-6-2-4, and the fuel is distributed evenly to each cylinder by the high-pressure common rail fuel injection system. The impact vibration test bench includes a impact vibration system, a coolant circulation system and a high-speed photography system, as shown in Figure 2(a).

In order to capture the cavitation phenomenon during vibration, an observation window is installed on the crankcase, and the pressure sensor is fixed on the upper part of the window to accomplish the measurement of water pressure and the observation of cavitation. The specific installation method is shown in Fig. 2(b). The distance between the pressure sensor probe and the cylinder liner surface is 4.7mm. The acceleration sensor is installed on the inner wall of the liner, together with a dynamic pressure sensor at the same horizontal position. The

vibration exciter drives the impact device to impose pulse excitation and sinusoidal excitation on the inner surface of the

liner to obtain the vibration and coolant pressure at the corresponding position.

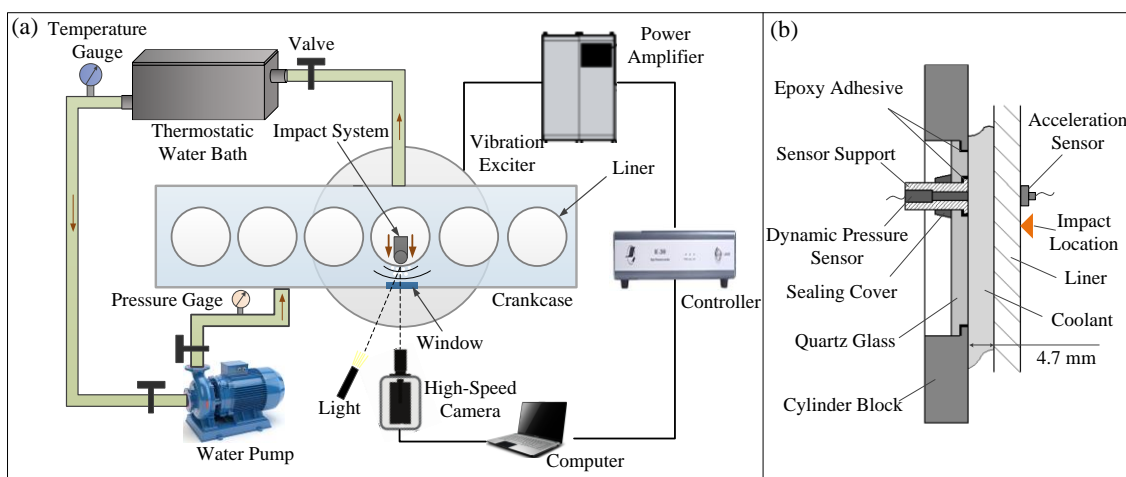


Fig.2. Diagram of the experimental setup. (a) Impact vibration test system. (b) Sensor installation diagram.

### 3.2 Boundary conditions of the dynamics model

Due to the complex structure of the heavy-duty diesel engine, only the high-precision regions are finely modeled to reduce the computational load. Specifically, the piston, cylinder liner and crankcase are finely modeled to ensure that their structure and modal characteristics are consistent with reality. The piston pin, connecting rod, and cylinder head are simplified, while the crankshaft is modeled as a rigid body. In the dynamics model, fixed joints and clearance fits are modeled by constructing a series of frictional contact pairs, which are solved using augmented Lagrangian methods.

The cylinder liner material for this engine is boron cast iron, which is a widely used material for cylinder liners in heavy duty diesel engines. Its modulus of elasticity is  $1.4e+11$  Pa, Poisson's ratio is 0.26, and density is  $7200 \text{ kg/m}^3$ . The main boundary conditions of the model include combustion pressure, piston thermal deformation, and bolt preload of the cylinder head. Based on the rated engine operating conditions with a crankshaft speed of 1900 r/min, the engine combustion

pressure measured by the test is shown in Fig. 3. The thermal boundary conditions of the piston involved in the calculation are shown in Fig. 4. The preload force for the cylinder head of the engine is 150 Nm. Instead of applying elastohydrodynamic (EHD) to the contact model between the piston and the cylinder liner, the model uses contact stiffness coefficients and damping coefficients in this study.

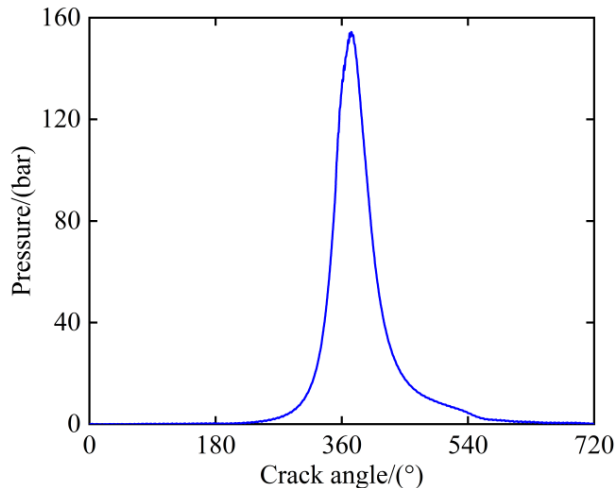


Fig.3. Measured combustion pressure curve.

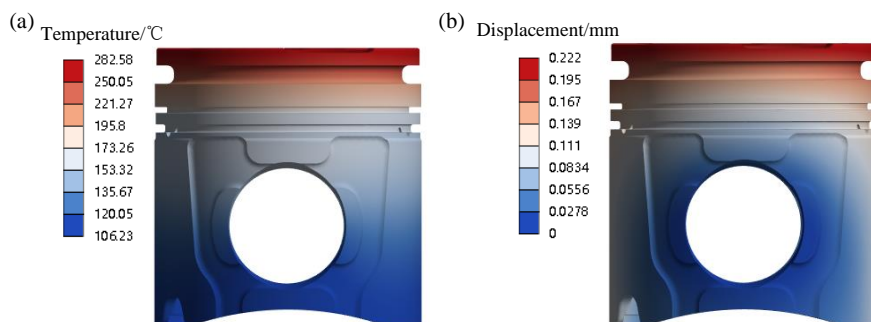


Fig.4. The piston thermal deformation parameters. (a) Temperature field; (b) Thermal deformation.

The finite element models of the crankcase and cylinder liner were established according to the actual structure, as shown in Fig. 5. In order to systematically study the distribution of liner vibration in different areas and cylinders, four analysis

nodes are set at 25mm intervals in the coolant area on the thrust side of the cylinder liner. The test measurement point is set at node 4 of the cylinder 1.

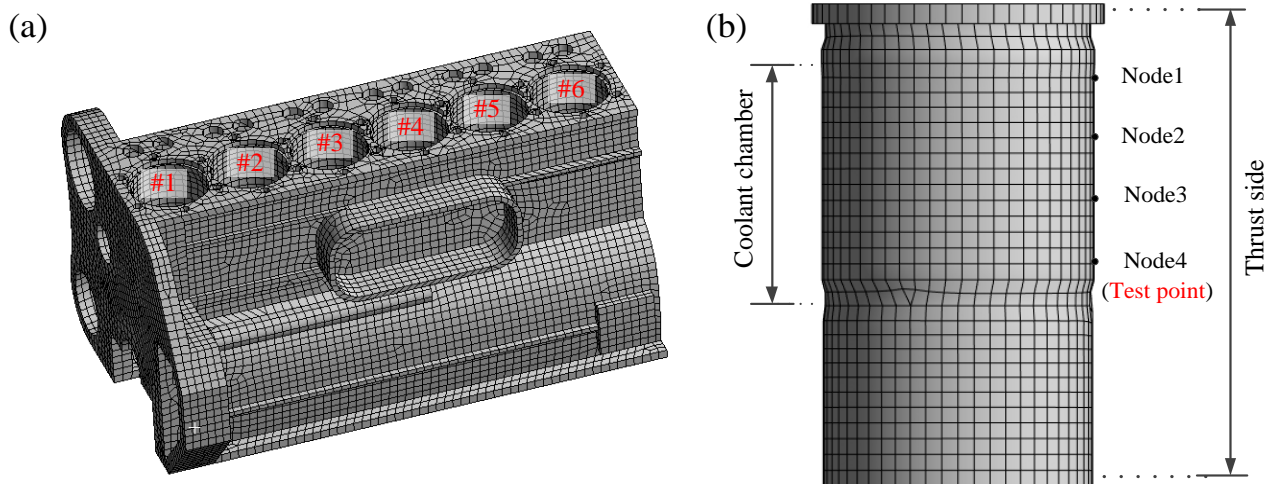


Fig.5. Finite element analysis model. (a) Crankcase; (b) Cylinder liner.

### 3.3. Frequency response analysis

Modal analysis is the basis of dynamics simulation. The cylinder liner and the crankcase are the two most critical components that affect vibration. In order to verify the accuracy

of the finite element model, the natural frequencies of the structural components are obtained by modal tests and compared with the simulated results, as shown in Fig. 6. The modal frequencies obtained from the test differed from the simulated results within 5%.

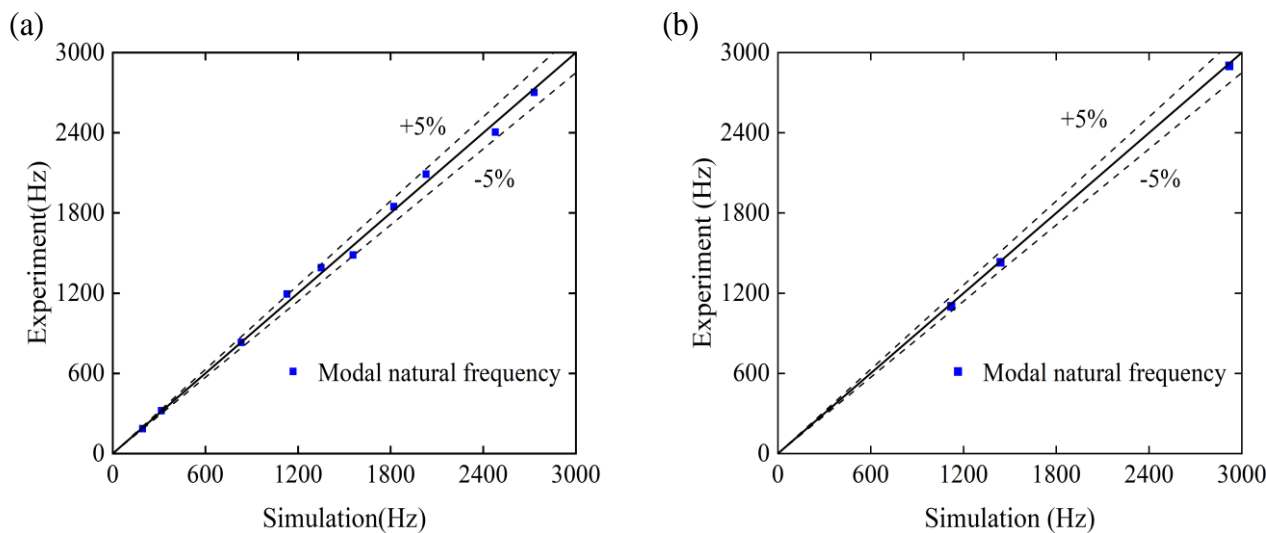


Fig.6. Simulated and measured modal natural frequency. (a) Crankcase; (b) Cylinder liner.

The frequency response function (FRF) is the ratio of response to excitation, which contains the modal and damping characteristics of the structure. In order to verify the damping characteristics of the structure, pulsed excitations are applied to the crankcase and cylinder liner to obtain simulated and measured acceleration signals at the same position. The FRF

results of the crankcase and cylinder liner are shown in Fig. 7. The simulated and measured frequency response distributions of the crankcase and cylinder liner are in good agreement, which indicates that the definition of structural damping characteristics is reasonable in this paper.

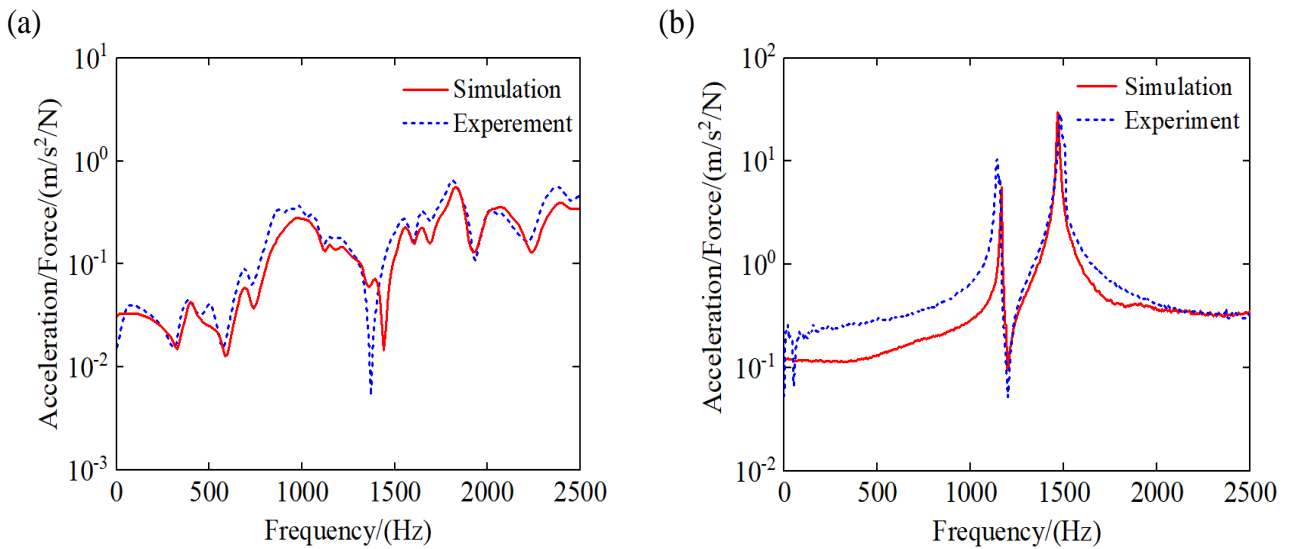


Fig.7. FRF results for the structure. (a) Crankcase; (b) Cylinder liner.

## 4. Results and discussion

### 4.1 Correspondence between liner vibration and coolant cavitation

Adjust the inlet and outlet conditions of the coolant system to keep the static pressure of the coolant close to the actual operating condition, and the static pressure is about 240 kPa. The liner vibration and coolant pressure fluctuation under

different excitation forces are measured by varying the exciter output power. The vibration and pressure under 50N and 800N excitation are shown in Fig. 8. When the excitation force is smaller, the acceleration waveform is in better agreement with the pressure waveform. Differently, when the excitation force is higher, the acceleration will complete the decay faster than the pressure.

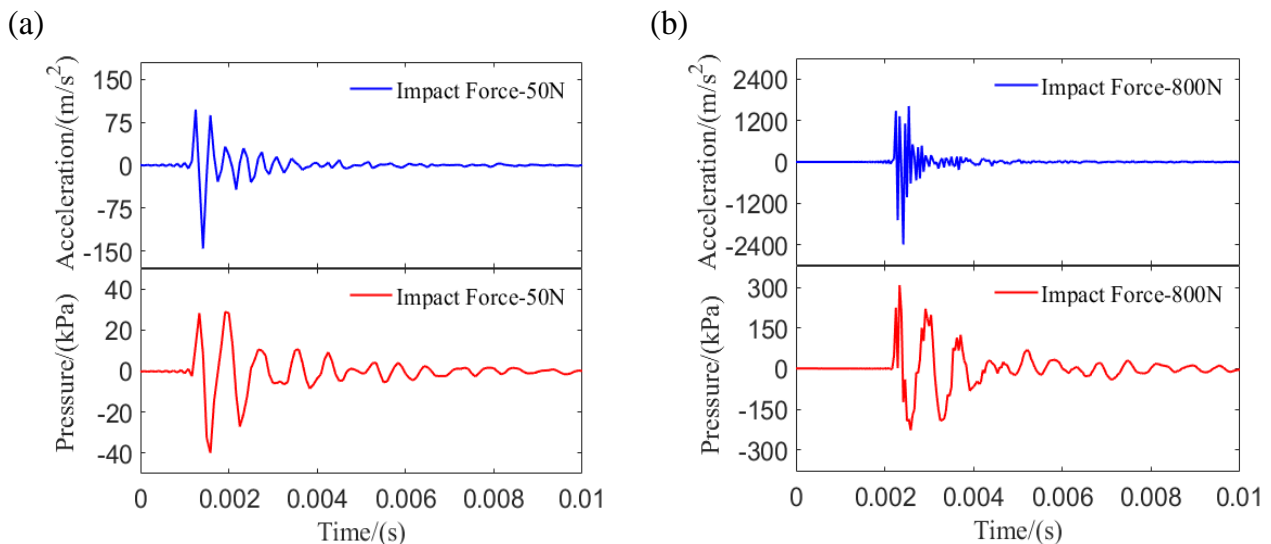


Fig.8. Measured acceleration and pressure waveforms under different impact forces. (a) Small impact force; (b) Large impact force.

The peak and valley values of coolant pressure during vibration are particularly noteworthy in the evaluation of cylinder liner cavitation. Fig. 9 shows the scatter plot of peak and valley values of acceleration and pressure for 260 pulse excitations. As shown by the linear regression curve in Fig. 9(a), the peak acceleration exhibits a good linear relationship with the

peak pressure. However, the negative acceleration has an obvious nonlinear relationship with the negative pressure, as shown in Fig. 9(b). It can be seen that the negative pressure gradually flattens with the increase of acceleration, which is caused by the cavitation of the coolant that weakens its wave-guiding ability.

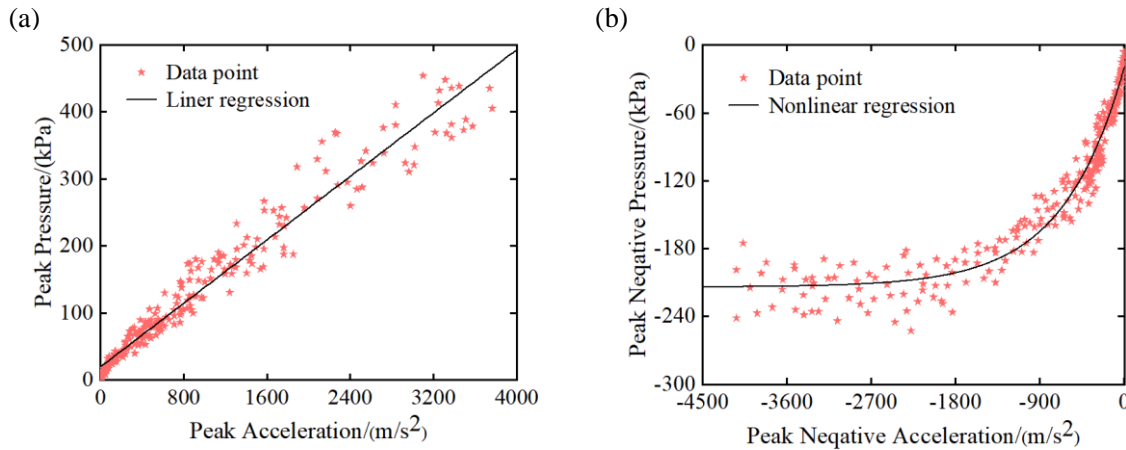


Fig.9. The relationship between cylinder liner acceleration and coolant pressure. (a) Positive peaks ;(b) Negative peaks.

Substitute the measured peak negative acceleration and peak negative pressure into Eq.11. The results of the acceleration-based cavitation evaluation at 90°C are shown in Figure 10. The horizontal axis is the absolute value of the peak negative acceleration, and the vertical axis is the remaining part of the Eq.11. The black solid line is plotted according to  $Ca = 1$ . When  $a$  is less than 917  $m/s^2$ ,  $Ca$  is always greater than 1, and the coolant does not reach cavitation conditions. When  $a$  is between 917  $m/s^2$  and 1189  $m/s^2$ ,  $Ca$  fluctuates around 1. When  $a$  is greater than 1189  $m/s^2$ ,  $Ca$  is always less than 1. Therefore, it can be considered that there is a higher risk of cavitation when the peak negative acceleration is greater than 1189  $m/s^2$ .

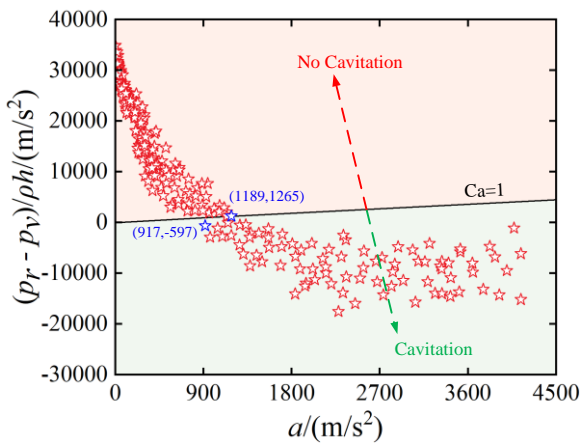


Fig.10. Phase diagram for cavitation based on acceleration.

Converting the cylinder liner acceleration measured by the impact vibration test into velocity by integration, the results of this study have been compared with the calculations based on empirical formulas, as shown in Fig. 11. The horizontal axis is the measured cylinder liner acceleration, and the vertical axis is the cylinder liner velocity calculated by integration. According to the *CSF* calculation in Eq. 7, cavitation will occur in the

coolant when the cylinder liner velocity exceeds  $V_{ccv}=0.11$  m/s. Correspondingly, when the acceleration exceeds 1920  $m/s^2$ , the data points are all located above the  $V_{ccv}=0.11$  m/s straight line. However, some of the data points with pressures below the saturation pressure had velocities below the threshold of  $V_{ccv}$ . Therefore, the cavitation state of the coolant cannot be accurately determined by  $V_{ccv}$ . This is because the thin liquid layer structure amplifies the pressure amplitude of the coolant, which lowers the vibration threshold for triggering cavitation. The ultrasonic cavitation test in the literature [9, 21] also demonstrates this phenomenon, which indicates that the *CSF*-based cavitation evaluation method is inaccurate in thin liquid layers. The cavitation evaluation method proposed in this paper considers the pressure gradient in the coolant thickness direction. Based on the reference pressure at the crankcase surface obtained by the impact vibration test, the pressure at the cylinder liner surface can be calculated more accurately by combining Eq. 9 and Eq. 10, thereby performing cavitation evaluation.

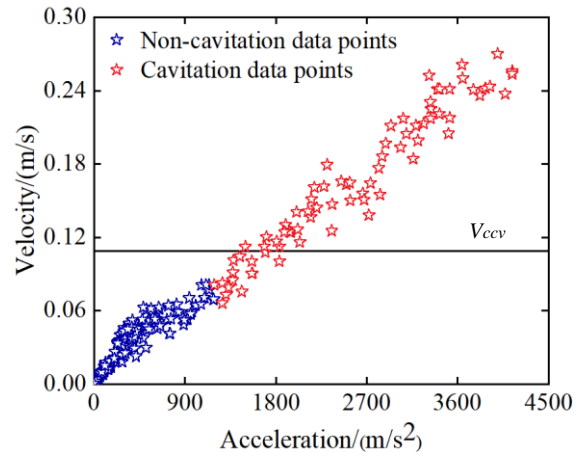


Fig.11. Comparison results of the two cavitation evaluation methods.

Cavitation conditions are photographed using a high-speed camera, with the excitation system imposing a sinusoidal excitation at a frequency of 100 Hz on the cylinder liner. The photographic field of view is a rectangle of 30 mm by 40 mm near the impact location, with a photographic speed of 10,000 fps and a photographic magnification of 0.5. Figure 12 shows the cavitation condition of the cylinder liner surface at the acceleration of  $1800 \text{ m/s}^2$ . The initial cavitation state is a tiny bubble nucleus, which develops continuously afterward.

Moreover, the development of cavitation shows aggregation, as shown by the three markers in Fig. 12(f). The bubbles enter the rupture phase after 0.6 ms, with the diameter of the bubble cluster and the number of vacuoles inside gradually decreasing until disappearance. It can be seen that a significant cavitation phenomenon has occurred when the cylinder liner vibration is below  $V_{ccv}$ , which further justifies the proposed method in this study.

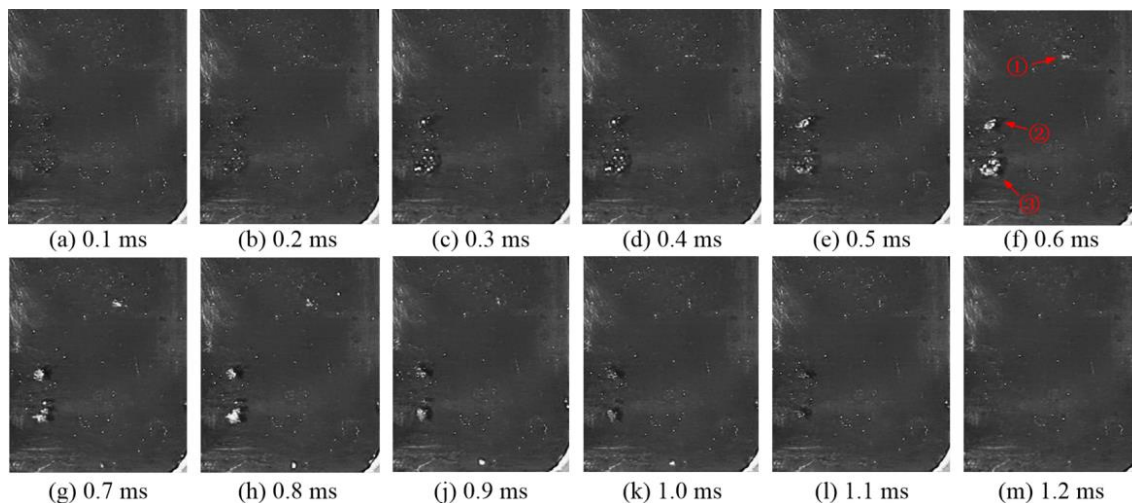


Fig.12. Cavitation patterns at sinusoidal excitation.

#### 4.2 Cavitation evaluation at different cylinders of the crankcase

Cavitation often occurs on the thrust side of the cylinder liner, but the location of cavitation varies from engine to engine in the axial direction of the liner. In addition, there is a difference in

the cavitation condition between the cylinders in multi-cylinder diesel engines.

The dynamic response of each cylinder under the piston slap is calculated, and the acceleration curve of each cylinder liner at the test point is shown in Fig. 13.

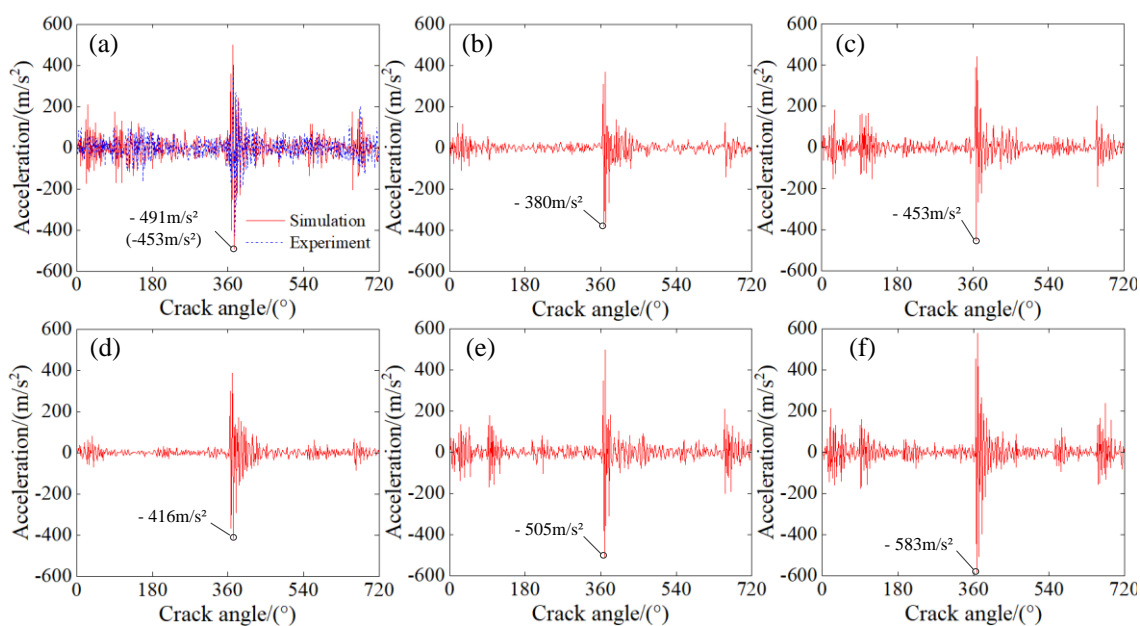


Fig.13. Acceleration response at the node 4. (a) Cylinder 1; (b) Cylinder 2; (c) Cylinder 3; (d) Cylinder 4; (e) Cylinder 5; (f) Cylinder 6.

Since the calculation does not consider the wrapping effect of coolant outside the cylinder liner, there is a 6% deviation between the simulated and measured values.

The peak negative acceleration of the four analysis nodes on the thrust side of cylinder liners is shown in Fig. 14.

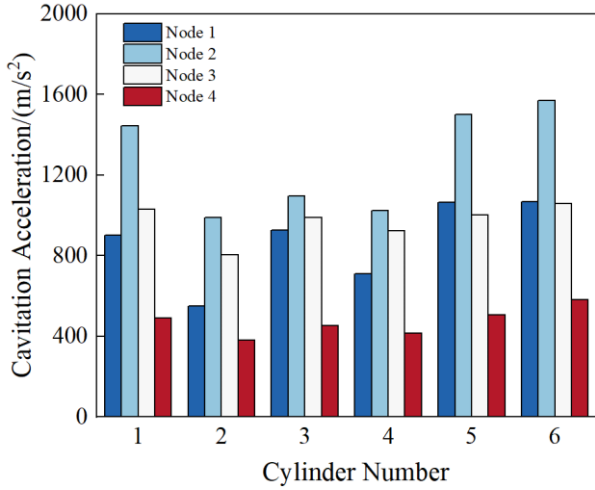


Fig.14. Acceleration distribution of six cylinders.

Under the same piston excitation, there is a significant difference in the peak negative acceleration of the six liners. The peak negative acceleration of cylinder 6 is the largest, followed by cylinder 5 and cylinder 1, and the peak negative acceleration of cylinder 2 is the smallest. In addition, the acceleration distribution trends of nodes in the six cylinders are similar, with the most intense vibration at node 2 and the least at node 4. The cylinder head bolt preload and the supporting effect of the

crankcase suppress the vibration in the top region of the cylinder liner. It leads to the peak acceleration located near node 2, where the structural stiffness is relatively low. Among the acceleration distributions of the six cylinders, the acceleration of cylinder 1, cylinder 5 and cylinder 6 at node 2 exceeded the cavitation threshold. In particular, cylinder 6 has the highest risk of cavitation with a peak negative acceleration of 1569 m/s<sup>2</sup>.

In order to analyze the differences in acceleration of different cylinders, the acceleration response spectra at node 4 for the six liners are calculated, as shown in Fig. 15. The peak frequency spectrum of all six cylinders is around 1850 Hz, which represents the modal frequency that has the greatest influence on the vibration. With the other boundary conditions identical, the acceleration differences of the six cylinders can be explained by the modal characteristics of the crankcase. The frequency of 1850Hz is close to the 7th-order modal natural frequency of the crankcase.

Fig. 16 shows the mode shape of the crankcase on the thrust side of six cylinders at 1874 Hz. The mode shape of the crankcase is largest in cylinder 6, followed by cylinder 5 and cylinder 1, which is consistent with the trend of acceleration distribution in Figure 14. The results show that there is a significant correlation between the vibration differences of each cylinder and the modal characteristics of the crankcase, and the cylinders with larger mode shape coefficients have a higher risk of cavitation.

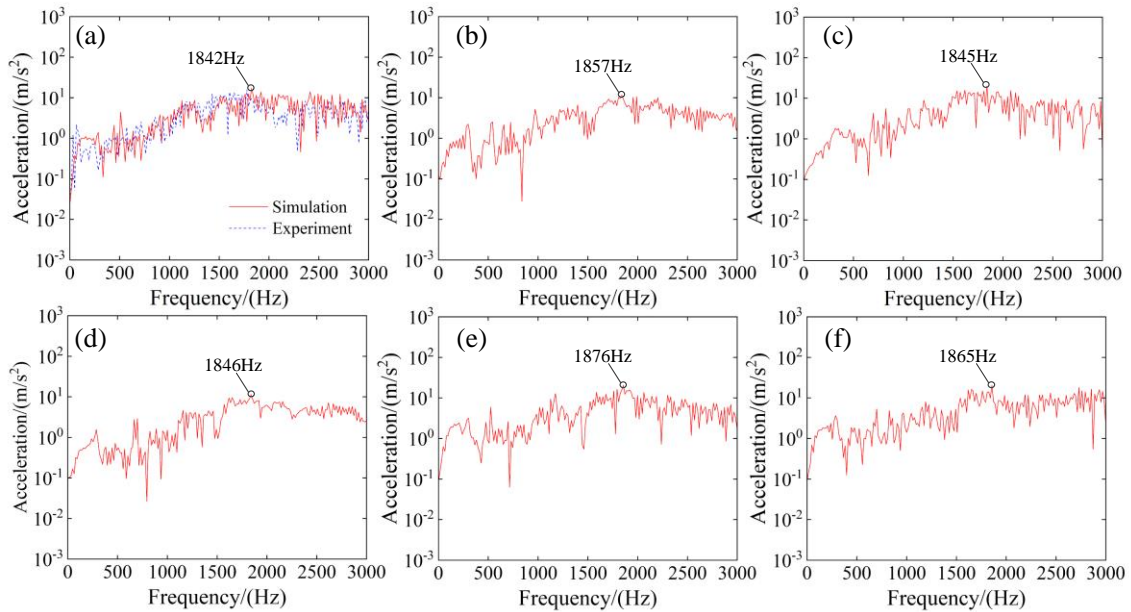


Fig.15. Frequency response of acceleration at the node 4. (a) Cylinder 1; (b) Cylinder 2; (c) Cylinder 3; (d) Cylinder 4; (e) Cylinder 5; (f) Cylinder 6.

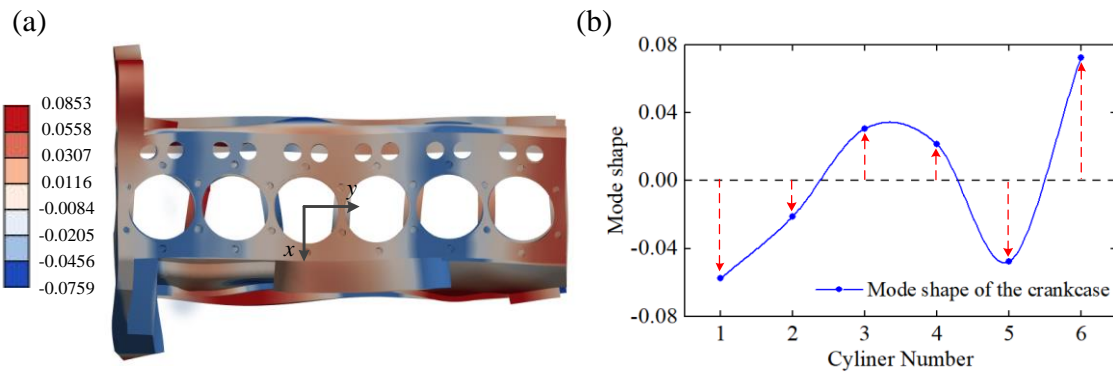


Fig.16. Mode shape of the crankcase in the direction of thrust at 1874 Hz. (a) Mode shape of the crankcase; (b) Mode shape of the crankcase on the thrust side.

### 4.3 Influence of clearance between piston and liner on cavitation

The cavitation behavior of the cylinder liner is a durability problem, and the cavitation failure usually occurs after working 1000 hours in actual cases. The piston skirt will be slightly worn in the process, which increases the clearance between the piston and the cylinder liner.

The cylinder liner vibration was calculated for cylinder 6 at different clearances, as shown in Figure 17.

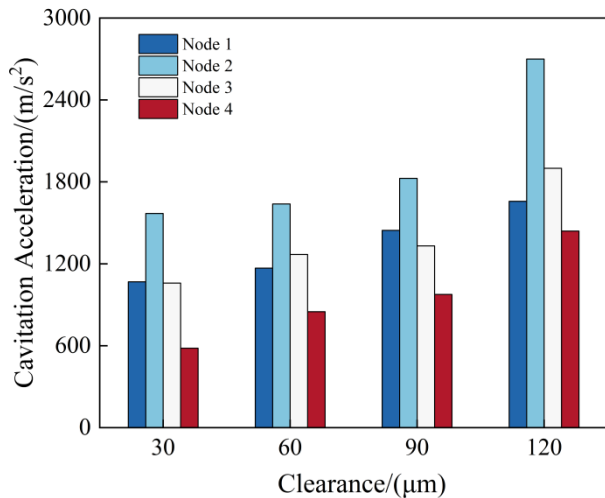


Fig.17. Acceleration of the cylinder liner at different clearances.

As the clearance increases, the vibration on the thrust side of the cylinder liner increases significantly. Especially when the clearance is 120 μm, the four areas on the thrust side of the cylinder liner are at risk of cavitation. Figure 18 shows the lateral displacement of the piston pin center at different clearances, where the coupling deformation of the piston and the cylinder liner is included in the results. The increase in clearance leads to a larger lateral displacement of the piston per unit time, resulting in an increase in the velocity of the lateral

movement and subsequently an increase in the impact kinetic energy. In addition, the increase in clearance will increase the piston rotation angle, resulting in a smaller contact area between the piston and the cylinder liner during the collision, thereby producing a sharper impact effect and further increasing the vibration of the cylinder liner. Moreover, the continuous increase in vibration can lead to an increase in cavitation and further reduce the life of the cylinder liner.

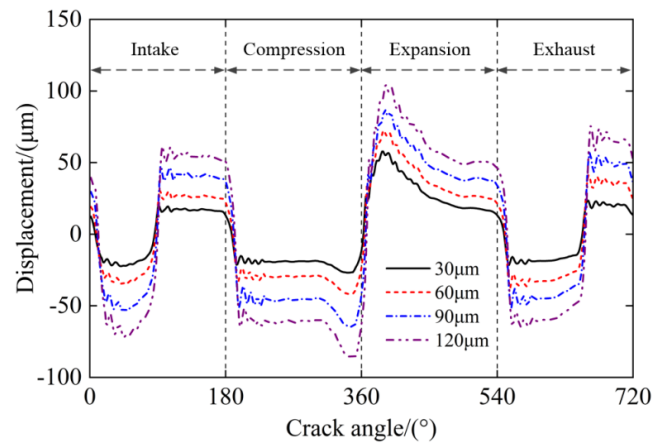


Fig.18. Lateral displacement of the piston at different clearances.

### 4.4 Influence of piston pin offset on cavitation

Optimizing the piston structure is a cost-saving and effective method in the design of diesel engines for cavitation suppression. The piston pin offset has a significant effect on the dynamic characteristics of the cylinder liner, but the influence regularities are variable in different engines due to the differences in piston structures. The contact force between the piston and the cylinder liner at different offsets is shown in Figure 19. The peak quasi-static force appears at 388.7°CA and increases gradually with the offset from -1 mm to 1 mm, as shown in Figure 19(a). The piston dynamic slap force shows

different trends, as shown in Figure 19(b). The peak piston dynamic slap force is greatest in the non-offset condition, and

both positive and negative offsets of the piston pin will weaken the piston dynamic slap force.

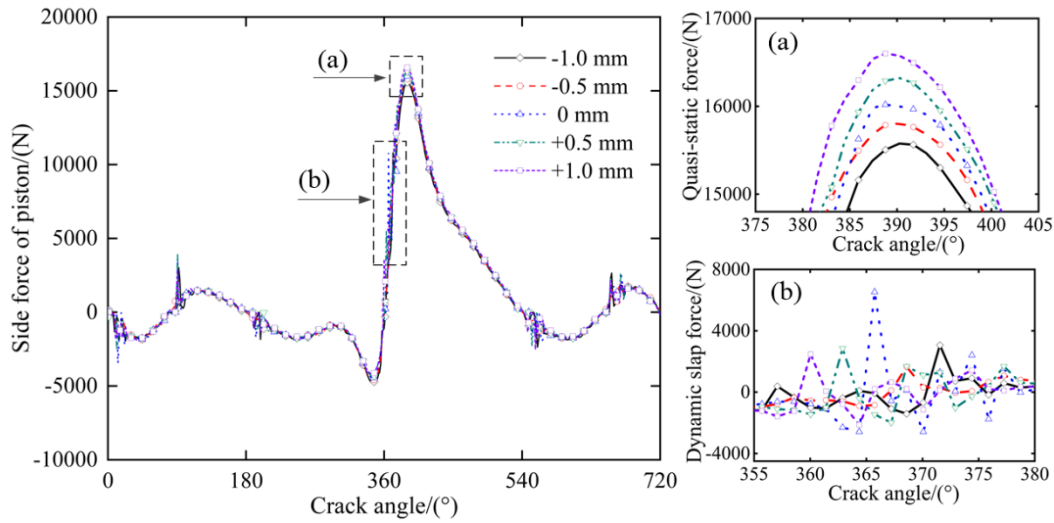


Fig.19. Piston side impact force at different offsets. (a) Quasi-static force; (b) Dynamic slap force.

Fig. 20 shows the rotation curve of the piston at different offsets. As the piston approaches the TDC, it rotates counterclockwise first and then clockwise. In the process of clockwise rotation, the piston moves towards the thrust side and imposes a slap force on the cylinder liner. When the offset is 0mm, the rotation angle of the piston is minimized, and it moves to the thrust side in approximately a translational manner. While in the offset condition, the rotation angle of the piston increases, with the top of the piston skirt contacting the cylinder liner first, followed by gradually coming into full contact with the cylinder liner as the piston rotates. Due to the low structural stiffness and relatively high elasticity of the piston skirt, it provides a buffering effect for the slapping action.

offsets. The peak negative acceleration of the cylinder liner decreases with the increase in positive offset. As the negative offset increases, the peak negative acceleration of the cylinder liner shows a trend of first decreasing and then increasing. Moreover, the trends of the peak negative acceleration at different offsets are consistent with the changes of dynamic slap force. Therefore, proper piston pin offset can effectively reduce vibration and cavitation without adding excessive frictional losses. When the offset is +1 mm, the decrease ratio of acceleration is the largest and the suppression of cavitation is the most significant.

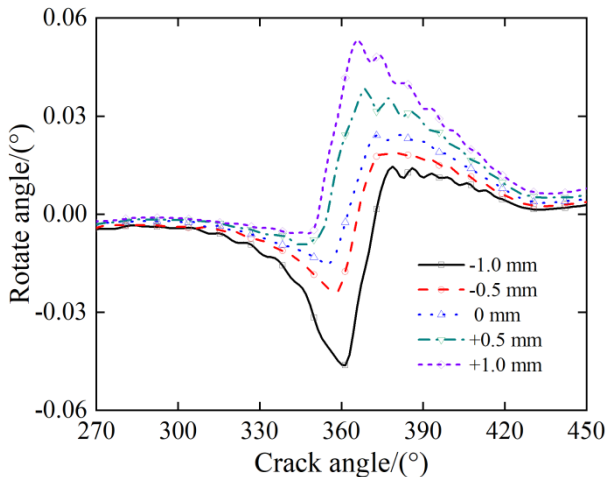


Fig.20. Rotation curve of the piston at different offsets.

Figure 21 shows the comparison of the peak negative acceleration on the thrust side of the cylinder liner at different

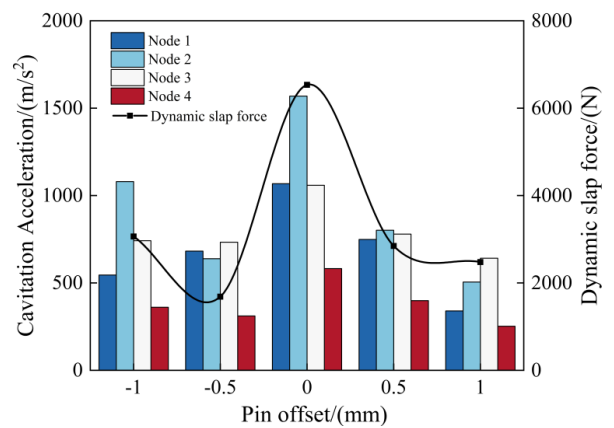


Fig.21. Acceleration of the cylinder liner at different offsets.

## 5. Conclusion

In this study, a novel approach is proposed to evaluate the cavitation risk of the cylinder liner under piston slap, which combines experimental analysis with the nonlinear structural

dynamics model to achieve the quantitative evaluation of the cavitation risk.

(1) The occurrence of cavitation will cause a nonlinear relationship between cylinder liner acceleration and coolant pressure, which can be used as an evaluation index of cavitation risk. The correspondence between vibration and cavitation has been further quantified through pressure gradient calculation and visualization observation, which is more accurate than the existing cavitation evaluation methods. The engine under study has a high risk of cavitation when the cylinder liner acceleration exceeds  $1189 \text{ m/s}^2$ .

(2) Accurate simulation of the dynamic behavior of the cylinder liner is critical for cavitation risk evaluation. A structural dynamics model is developed considering structural modal properties, nonlinear contact constraints and time-varying excitation forces. The cylinder liner vibration response calculated based on the dynamics model is in good agreement with the measured results, which provides a reliable basis for cavitation risk evaluation.

(3) Differences in cavitation risk of each cylinder in heavy-duty diesel engines are related to the modal characteristics of the crankcase. There is a higher cavitation risk in regions with

larger mode shape coefficients around the main vibration frequency of the crankcase. The risk of cavitation is highest for the cylinders located at the edge of an engine system, which is consistent with phenomena that have been observed during engine operation.

(4) There is a significant effect of piston-liner clearance and pin offset on the cavitation risk. Reducing the piston-liner clearance and proper piston pin offset can effectively reduce the cavitation risk of the cylinder liner.

The approach presented in this paper can quantitatively assess the cavitation risk of cylinder liners and guide the cavitation-resistant design of diesel engines in engineering practice. This paper investigates the dynamic response of the cylinder liner under one operating condition of the engine. Other operating parameters can be further considered in the future, including speed, torque, etc. In addition, to improve the accuracy of the cavitation risk assessment model, it is also necessary to consider the effects of flow field characteristics such as flow velocity, surface tension, and vacuole collapse energy on cavitation erosion. This is an ongoing question that we will continue to address in future work.

## Acknowledgments

This work was supported by the National Natural Science Foundation of China (NO. 51805353) and Research Project Supported by Shanxi Scholarship Council of China (NO. HGKY2019041).

## References

1. Abreu M, Sundberg J, Elfsberg J, et al. Morphology and mechanisms of cavitation damage on lamellar gray iron surfaces[J]. *Wear*, 2020, 456: 203324, <https://doi.org/10.1016/j.wear.2020.203324>.
2. Antkowiak A, Bremond N, Le Dizes S, et al. Short-term dynamics of a density interface following an impact[J]. *Journal of Fluid Mechanics*, 2007, 577: 241-250, <https://doi.org/10.1017/s0022112007005058>.
3. Bai L, Yan J, Zeng Z, et al. Cavitation in thin liquid layer: A review[J]. *Ultrasonics Sonochemistry*, 2020, 66: 105092, <https://doi.org/10.1016/j.ultsonch.2020.105092>.
4. Bako S, Nasir A, Ige B, et al. Cavitation deterioration of diesel power plant cylinder liner[J]. *Journal of Mechanical and Energy Engineering*, 2020, 4(3): 239-246, <https://doi.org/10.30464/jmee.2020.4.3.239>.
5. Bezyukov O K, Zhukov V A, Pulyaev A A. Criteria for calculating cavitation erosion in cooling systems for internal combustion engines[C]//AIP Conference Proceedings. AIP Publishing LLC, 2022, 2647(1): 060010, <https://doi.org/10.1063/5.0118556>.
6. Brennen C E. Cavitation and bubble dynamics[M]. Cambridge university press, 2014, <https://doi.org/10.1017/CBO9781107338760>
7. Dolatabadi N, Theodossiades S, Rothberg S J. On the identification of piston slap events in internal combustion engines using tribodynamic analysis[J]. *Mechanical Systems and Signal Processing*, 2015, 58: 308-324, <https://doi.org/10.1016/j.ymssp.2014.11.012>.
8. Dong, Hong-Quan; Dynamic modeling and cavitation tendency analysis of cylinder liner considering the effects of moving loads[J]. *Transactions of Csice*, 2013, Vol.31(5): 467-472.
9. Fatjó G G A, Pérez A T, Hadfield M. Experimental study and analytical model of the cavitation ring region with small diameter ultrasonic

- horn[J]. *Ultrasonics sonochemistry*, 2011, 18(1): 73-79. <https://doi.org/10.1016/j.ultsonch.2009.12.006>.
10. Fontanesi S, Giacomini M, Cicalese G, et al. Numerical investigation of the cavitation damage in the wet cylinder liner of a high performance motorbike engine[J]. *Engineering Failure Analysis*, 2014, 44: 408-423, <https://doi.org/10.1016/j.engfailanal.2014.05.025>.
  11. Geng Z, Chen J. Investigation into piston-slap-induced vibration for engine condition simulation and monitoring[J]. *Journal of sound and vibration*, 2005, 282(3-5): 735-751, <https://doi.org/10.1016/j.jsv.2004.03.057>.
  12. Gomboc S, Cristofaro M, Haramincic B, et al. Cavitation Erosion Prediction at Vibrating Walls by Coupling Computational Fluid Dynamics and Multi-body-Dynamic Solutions[J]. *SAE International Journal of Commercial Vehicles*, 2021, 14(02-14-03-0021): 259-270, <https://doi.org/10.4271/02-14-03-0021>.
  13. Hosny D M, Young R W, Engineering Mechanics Seniors. A system approach for the assessment of cavitation corrosion damage of cylinder liners in internal combustion engines[J]. *SAE Transactions*, 1993: 699-715, <https://doi.org/10.4271/930581>.
  14. Javanmardi D, Rezvani M A. Thermomechanical Fracture Failure Analysis of a Heavy-Duty Diesel Engine Cylinder Liner through Performance Analysis and Finite Element Modeling[J]. *SAE International Journal of Engines*, 2020, 13(5): 665-684, <https://doi.org/10.4271/03-13-05-0042>.
  15. Krechetnikov R. Flow around a corner in the water impact problem[J]. *Physics of Fluids*, 2014, 26(7): 072107, <https://doi.org/10.1063/1.4891229>.
  16. Li G, Gu F, Wang T, et al. Investigation into the vibrational responses of cylinder liners in an IC engine fueled with biodiesel[J]. *Applied Sciences*, 2017, 7(7): 717, <https://doi.org/10.3390/app7070717>.
  17. Lin L J. An Analysis of the Factors Influencing Cavitation in the Cylinder Liner of a Diesel Engine[J]. *Fluid Dynamics & Materials Processing*, 2022, 18(6):1667-1682, <http://doi.org/10.32604/fdmp.2022.019768>.
  18. Liu H, Wang X, Wu Y, et al. Effect of diesel/PODE/ethanol blends on combustion and emissions of a heavy duty diesel engine[J]. *Fuel*, 2019, 257: 116064, <https://doi.org/10.1016/j.fuel.2019.116064>.
  19. Lowe A S H. An Analytical Technique for Assessing Cylinder Liner Cavitation Erosion[J]. *SAE Transactions*, 1990: 439-448, <https://doi.org/10.4271/900134>.
  20. Meng F M, Wang X F, Li T T, et al. Influence of cylinder liner vibration on lateral motion and tribological behaviors for piston in internal combustion engine[J]. *Proceedings of the Institution of Mechanical Engineers, Part J: Journal of Engineering Tribology*, 2015, 229(2): 151-167, <https://doi.org/10.1177/1350650114545140>.
  21. Moussatov A, Granger C, Dubus B. Ultrasonic cavitation in thin liquid layers[J]. *Ultrasonics sonochemistry*, 2005, 12(6): 415-422, <https://doi.org/10.1016/j.ultsonch.2004.09.001>.
  22. Murakami H, Nakanishi N, Ono N, et al. New three-dimensional piston secondary motion analysis method coupling structure analysis and multi body dynamics analysis[J]. *SAE International Journal of Engines*, 2012, 5(1): 42-50, <https://doi.org/10.4271/2011-32-0559>.
  23. Nouri J M, Vasilakos I, Yan Y. Cavitation between cylinder-liner and piston-ring in a new designed optical IC engine[J]. *International Journal of Engine Research*, 2022, 23(7): 1144-1158, <https://doi.org/10.1177/14680874211008007>.
  24. Ohta K, Wang X, Saeki A. Piston slap induced pressure fluctuation in the water coolant passage of an internal combustion engine[J]. *Journal of Sound and Vibration*, 2016, 363: 329-344, <https://doi.org/10.1016/j.jsv.2015.10.026>.
  25. Pan Z, Kiyama A, Tagawa Y, et al. Cavitation onset caused by acceleration[J]. *Proceedings of the National Academy of Sciences*, 2017, 114(32): 8470-8474. <https://doi.org/10.1073/pnas.1702502114>.
  26. Peiyu X, Daojing G, Guannan H, et al. Influence of piston pin hole offset on cavity erosion of diesel engine cylinder liner[J]. *Engineering Failure Analysis*, 2019, 103: 217-225, <https://doi.org/10.1016/j.engfailanal.2019.04.022>.
  27. Pogodaev L I, Tret'Yakov D V, Valishin A G, et al. Simulation of durability of cylinder liners of an internal combustion engine under vibration cavitation[J]. *Journal of Machinery Manufacture and Reliability*, 2008, 37(2): 143-151, <https://doi.org/10.3103/s105261880802009x>.
  28. Shi Z, Cao W, Wu H, et al. Research on destructive knock combustion mechanism of heavy-duty diesel engine at low temperatures[J]. *Combustion Science and Technology*, 2022: 1-24, <https://doi.org/10.1080/00102202.2022.2156790>.
  29. Steck B. Avoiding cavitation on wet cylinder liners of heavy duty diesel engines by parameter changes[C]//2008 SAE Brasil Congress and Exhibit. 2008 (2008-36-0073), <https://doi.org/10.4271/2008-36-0073>.

30. Tsujiuchi N, Koizumi T, Hamada K, et al. Optimization of profile for reduction of piston slap excitation[J]. SAE transactions, 2004: 1773-1780, <https://doi.org/10.4271/2004-32-0022>
31. Um D. Finite Element Modeling and Analysis: Practical Application[J]. Solid Modeling and Applications: Rapid Prototyping, CAD and CAE Theory, 2018: 297-324. [https://doi.org/10.1007/978-3-319-74594-7\\_9](https://doi.org/10.1007/978-3-319-74594-7_9).
32. Wang X, Ohta K. Study on piston slap induced liner cavitation[J]. Journal of Vibration and Acoustics, 2015, 137(5), <https://doi.org/10.1115/1.4030360>.
33. Wang X, Wang H, Zhao J, et al. Evaluation of Liner Cavitation Potential through Piston Slap and BEM Acoustics Coupled Analysis[J]. Mathematics, 2022, 10(6): 853, <https://doi.org/10.3390/math10060853>.
34. Wang X, Zhang Z, Li Y. Analysis of water coolant pressure fluctuation induced by piston slap[J]. Engineering Failure Analysis, 2020, 112: 104382, <https://doi.org/10.1016/j.engfailanal.2020.104382>.
35. Wu L, Bi Y, Shen L, et al. Study on the effect of piston skirt profile on the vibration behavior of non-road high pressure common rail diesel engine[J]. Applied Acoustics, 2019, 148: 457-466, <https://doi.org/10.1016/j.apacoust.2019.01.007>.
36. Zhang B, Zhang P, Guo X, et al. simulation Research on Cavitation Flow Characteristics of Highly Enhanced Diesel Engine Cooling System[C]//Iop Conference Series: Earth And Environmental Science. IOP Publishing, 2019, 237(4): 042017, <http://doi.org/10.1088/1755-1315/237/4/042017>.